11a) that is metastable with respect to dissociation to C_2H_4 and CO. Vertical neutralization of $1^{\bullet+}$ forms a vibrationally excited 1 of ca. 40 kJ mol^{-1} internal energy. According to previous ab initio calculations[3b] such excitation alone is insufficient to bring about isomerization to 2, consistent with our neutralization–reionization experiments. Cyclopropanone 2 is calculated to be an equilibrium structure (Figure 11b), metastable with respect to dissociation to C_2H_4 and CO, but more stable than 1. The standard heat of formation of 2 (Table IV), calculated relative to 13 including the 0 K relative energies and 298 K heat contents, is in reasonable agreement with the previous measurements[8] and estimates.[4]

The calculations further predict that the $^{\bullet}CH_2CH_2CO^{\bullet}$ biradical produced by neutralization of $4^{\bullet+}$ should be a high-energy species. Dissociation of the $^{\bullet}CH_2CH_2CO^{\bullet}$ singlet to C_2H_4 and CO is predicted to be highly exothermic, consistent with the observed instability of the neutral 4 and the further dissociations of the primary C_2H_4 and CO fragments. The calculated large energy difference between the neutralized singlet and triplet states reflects the different extent of vibrational perturbation upon vertical neutralization rather than the actual singlet–triplet gap in relaxed $^{\bullet}CH_2CH_2CO^{\bullet}$ biradicals.[51] Interestingly, the energy of the $^{\bullet}CH_2CH_2CO^{\bullet}$ triplet is above the threshold for the $CH_2{=}C{=}O$ and CH_2 formation (400 kJ mol^{-1} above C_2H_4 + CO). This may explain the observed competition between these two dissociation channels in a fraction of neutralized 4. In contrast to 4, neutralization of $14^{\bullet+}$ produces an unbound $C_2H_4\cdots OC$ complex, which dissociates without barrier to its components. Due to the calculated low exothermicity (10.5 kJ mol^{-1}) for the latter reaction, it should not show a large kinetic energy release as was observed for the dissociations of 4.

Conclusions

The experimental and theoretical studies demonstrate that methyleneoxirane ($1^{\bullet+}$) and $^{\bullet}CH_2CH_2CO^{+}$ ($4^{\bullet+}$) cation radicals are stable species that undergo only limited degenerate isomerizations on collisional activation. The cyclopropanone ion, $2^{\bullet+}$, is unstable and functions as a transition state for the degenerate isomerization of $4^{\bullet+}$. The oxyallyl cation radical ($3^{\bullet+}$) is only marginally stable, and appears as an intermediate in the degenerate isomerization of $1^{\bullet+}$ and in the dissociative ionization of diketene (12). The neutral molecules 1 and 2 are stable species. Neutralization of $4^{\bullet+}$ yields $^{\bullet}CH_2CH_2CO^{\bullet}$ biradicals that decompose within 1 μs. The singlet state is assumed to collapse to C_2H_4 and CO, while the triplet forms $CH_2{=}C{=}O$ and $(^3B_2)CH_2$ in a competing dissociation.

Acknowledgment. We gratefully acknowledge the generous financial support of the National Science Foundation (Grant CHE-8712039) and, for partial instrument funding, the National Institutes of Health (GM16609) and the computational support and technical assistance of the Cornell National Supercomputer Facility, which receives major funding from the National Science Foundation and the IBM corporation, with additional support from New York State and the Corporate Research Institute.

Supplementary Material Available: Table of calculated harmonic vibrational frequencies (2 pages). Ordering information is given on any current masthead page.

---

(51) Borden, W. T.; Ed. *Diradicals*; Wiley-Interscience: New York, 1982.

Gas-Phase Formation and Rearrangements of Methyloxirene and Its Cation Radical

Frantisek Turecek,*,† Donald E. Drinkwater, and Fred W. McLafferty*

Contribution from the Department of Chemistry, Baker Laboratory, Cornell University, Ithaca, New York 14853-1301. *Received December 10, 1990*

Abstract: The gas-phase loss of N_2 from ionized diazoacetone generates the methyloxirene cation radical ($1^{\bullet+}$), not ionized methylformylcarbene ($2^{\bullet+}$) or acetylcarbene ($3^{\bullet+}$), as determined by collisionally activated dissociation (CAD) and charge-inversion mass spectra and isotopic labeling. Vertical neutralization of $1^{\bullet+}$ by charge exchange with mercury atoms produces neutral methyloxirene (1) that is unstable, rearranging mainly to methylketene and 2-propenal or 1-hydroxypropyne via 2. This mechanism supports that of Zeller for the corresponding solution photochemistry of the Wolff rearrangement, in contrast to that proposed for the gaseous photochemistry. Semiempirical AM1 and ab initio (MP4/6-31G*//3-21G) calculations predict 1, 2, and 3 to exist in potential energy minima separated by low isomerization barriers.

Simple oxirenes represent a class of highly strained antiaromatic heterocycles whose high reactivity has made isolation or direct detection difficult.[1] Methyloxirene (1) has been proposed as the key intermediate in the Wolff rearrangement[2] of 2-diazopropanal[3] and diazoacetone,[3,4] interconnecting methylformylcarbene (2) and acetylcarbene (3), which competitively rearrange to methylketene (4, Scheme I, routes d and e). On the basis of ^{13}C label distribution in chemically trapped 4 produced by solution photolysis of [1-^{13}C]-diazoacetone and [1-^{13}C]-2-diazopropanal, Zeller[3] concluded that hydrogen migration, route e, is predominant in 4 formation. In contrast, the gas-phase photolysis of 2-^{13}C-diazoacetone to yield mostly ^{13}CO was interpreted to occur by predominant 3 → 4 methyl migration, route d.[4] Dimethyloxirene (for which routes d and e are identical) has been identified as a minor product of the photolysis of $CH_3COCN_2CH_3$ at 25 K in a rare gas matrix, isomerizing with an activation energy of ~8 kJ mol^{-1} to $O{=}C{=}C(CH_3)_2$ (more abundant) and $CH_2{=}CHCOCH_3$ (homologues of 4 and 5).[5] Other conceivable pathways, not considered in the previous studies,[3,4] include methyl migration to oxygen in

---

† Present address: Department of Chemistry, University of Washington, Seattle, WA 98195.

(1) For a review on oxirenes see: Lewars, E. G. *Chem. Rev.* **1983**, *83*, 519–534.

(2) Wolff, L. *Liebigs Ann. Chem.* **1902**, *325*, 129.

(3) Zeller, K.-P. *Liebigs Ann. Chem.* **1979**, 2036–2042.

(4) Fenwick, J.; Fater, G.; Ogi, K.; Strausz, O. P. *J. Am. Chem. Soc.* **1973**, *95*, 124–132.

(5) (a) Debu, F.; Monnier, M.; Verlaque, P.; Davidovics, G.; Pourcin, J.; Bodot, H.; Aycard, J.-P. *C.R. Acad. Sci. Paris, Ser. 2* **1986**, *303*, 897–902. (b) Bachmann, C.; N'Guessan, T. Y.; Debu, F.; Monnier, M.; Pourcin, J.; Aycard, J.-P.; Bodot, H. *J. Am. Chem. Soc.* **1990**, *112*, 7488–7497.

0002-7863/91/1513-5958$02.50/0 © 1991 American Chemical Society

Scheme I

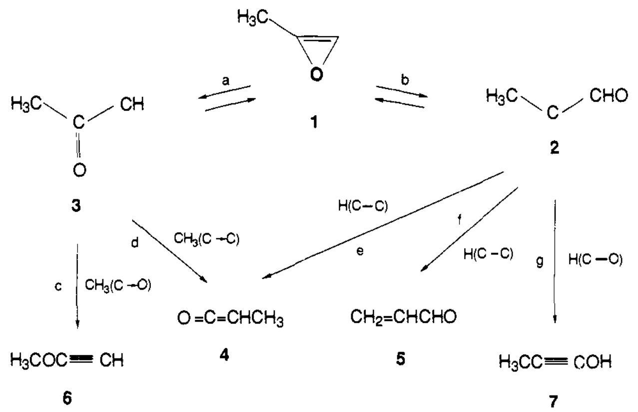

3 to form methoxyacetylene (**6**, route c) and hydrogen migrations in **2** yielding 2-propenal (**5**, route f) or 1-hydroxypropyne (**7**, route g). Theoretical calculations of the potential energy surface for isomerizations of the parent oxirene have been reported, estimating its isomerization activation energy as ~8 kJ mol^{-1}.[6]

The Wolff rearrangement of diazoketone cation radicals derived from diazoacetophenone,[7a] 2-diazo-1-oxonaphthalene,[7b] 1-diazo-3-phenoxypropan-2-one,[7c] and 1-diazo-4-(tosylamino)butan-2-one[7d] has been investigated, though no evidence for oxirene intermediates has been found. On the other hand, the parent oxirene cation radical has been generated recently by dissociative ionization of isoxazole, oxazole, and vinylidene carbonate[8] and shown to be a stable species as predicted earlier by ab initio theoretical calculations.[9]

This paper presents evidence that the stable methyloxirene cation radical ($\mathbf{1}^{\bullet+}$) is generated by dissociative ionization of diazoacetone in the gas phase. Neutral **1** is formed from $\mathbf{1}^{\bullet+}$ and characterized by neutralization–reionization mass spectrometry (NRMS);[10] NRMS produced the parent oxirene only as an unstable species.[8] To aid in the interpretation of the experimental data, the relative stabilities and isomerization barriers of the **1**, **2**, and **3** neutrals and cation radicals are assessed by semiempirical and ab initio calculations.

Experimental Section

Measurements were made with a tandem mass spectrometer described previously consisting of a modified Hitachi RMH-2 double-focusing mass spectrometer as the first mass analyzer (MS-I), a special collision region furnished with three collision cells, an electrostatic analyzer (ESA-II) as MS-II, and a second magnet as MS-III.[11] For $^{+}\text{NR}^{+}$ mass spectra the ions produced at 70 eV electron energy and accelerated to 9.9 keV are selected by MS-I and allowed to undergo charge-exchange neutralization with Hg vapor at 70% transmittance in the first collision cell.[12] The remaining ions are deflected electrostatically, and the resulting fast neutrals are reionized with oxygen at 50% transmittance in the second collision cell.[13] For $^{+}\text{NCR}^{+}$ mass spectra, the selected neutrals exiting from the first collision cell undergo collisions with helium (50% transmittance) in the second collision cell; the ions formed are deflected electrostatically, and the remaining neutrals reionized by collisions with oxygen (50% transmittance) in the third collision cell. For charge reversal ($^{+}\text{NR}^{-}$) experiments, benzene (25% transmittance) was used as a single target gas in the second collision cell. For MS/MS/MS experiments,[10f,11b] the ions undergo collisions with oxygen (50% transmittance) in the third field-free region, are selected by ESA-II, and are allowed to collide with helium (50% transmittance) in the fourth field-free region, and the CAD products are analyzed by the second magnet.

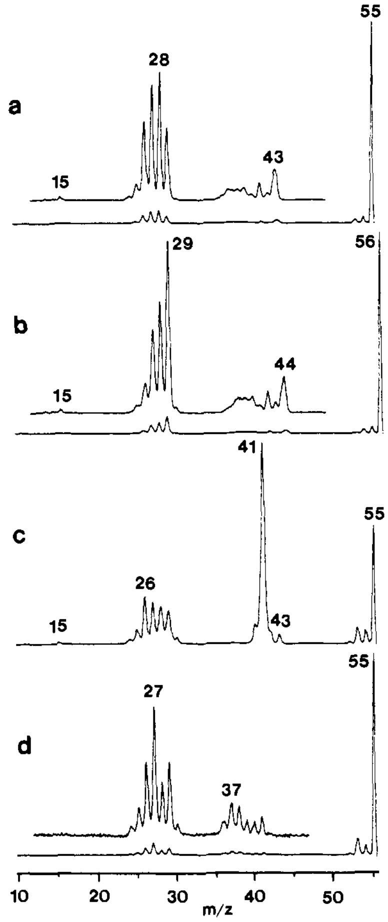

Figure 1. CAD/O_2 spectra of (a) $\mathbf{1}^{\bullet+}$, (b) $(\mathbf{1}\text{-}^{13}\text{C})^{\bullet+}$, (c) $\mathbf{6}^{\bullet+}$, and (d) $\mathbf{7}^{\bullet+}$.

Calculations. Standard ab initio molecular orbital calculations were carried out with use of the GAUSSIAN 88 program.[14] Geometry optimizations were performed with the HF/3-21G and HF/6-31G* basis sets. Harmonic vibrational frequencies, calculated at the HF/3-21G level, were used both to characterize stationary points on the surface as minima (all frequencies real, representing equilibrium structures) or first-order saddle points (one imaginary frequency, representing transition structures) and (after scaling by 0.9) to calculate zero-point vibrational contributions to relative energies. Improved relative energies were obtained through calculations on the HF/3-21G optimized geometries with use of Møller–Plesset perturbation theory[15] terminated at second (MP2), third (MP3), and fourth (MP4) orders. Our best theoretical relative energies correspond to MP4/6-31G* values, together with the zero-point vibrational corrections. Unless stated otherwise, these are the values referred

---

[6] Strausz, O. P.; Gosavi, R. K.; Denes, A. S.; Czismadia, I. G. *J. Am. Chem. Soc.* **1976**, *98*, 4784–4786. Tanaka, K.; Yoshimine, M. *J. Am. Chem. Soc.* **1980**, *102*, 7655–7662. Bouma, W. J.; Nobes, R. H.; Radom, L.; Woodward, C. E. *J. Org. Chem.* **1982**, *47*, 1869–1875. Schroder, S.; Thiel, W. *J. Am. Chem. Soc.* **1986**, *108*, 7985–7989.

[7] (a) Thomas, C. W.; Leveson, L. L. *Org. Mass Spectrom.* **1978**, *13*, 39–42. (b) Zeller, K.-P. *Org. Mass Spectrom.* **1975**, *10*, 317–319. (c) Selva, A.; Ferrario, F.; Saba, A. *Org. Mass Spectrom.* **1987**, *22*, 189–196. (d) Selva, A.; Saba, A. *Org. Mass Spectrom.* **1989**, *24*, 27–30.

[8] Hop, C. E. C. A.; Holmes, J. L.; Terlouw, J. K. *J. Am. Chem. Soc.* **1989**, *111*, 441–445.

[9] Bouma, W.; Gill, P. M. W.; Radom, L. *Org. Mass Spectrom.* **1984**, *19*, 610–616.

[10] (a) Gellene, G. I.; Porter, R. F. *Acc. Chem. Res.* **1983**, *16*, 200–207. (b) Danis, P. O.; Wesdemiotis, C.; McLafferty, F. W. *J. Am. Chem. Soc.* **1983**, *105*, 7454–7457. For recent reviews see: (c) Wesdemiotis, C.; McLafferty, F. W. *Chem. Rev.* **1987**, *87*, 485–500. (d) Terlouw, J. K.; Schwarz, H. *Angew. Chem., Int. Ed. Engl.* **1987**, *26*, 805–815. (e) Holmes, J. L. *Mass Spectrom. Rev.* **1989**, *8*, 513–539. (f) McLafferty, F. W.; Wesdemiotis, C. *Org. Mass Spectrom.* **1989**, *24*, 663–668. (g) McLafferty, F. W. *Science* **1990**, *247*, 925–929.

[11] (a) McLafferty, F. W.; Todd, P. J.; McGilvery, D. C.; Baldwin, M. A. *J. Am. Chem. Soc.* **1980**, *102*, 3360–3363. (b) Feng, R.; Wesdemiotis, C.; Baldwin, M. A.; McLafferty, F. W. *Int. J. Mass Spectrom. Ion Proc.* **1988**, *86*, 95–107.

[12] Danis, P. O.; Feng, R.; McLafferty, F. W. *Anal. Chem.* **1986**, *58*, 348–354.

[13] Danis, P. O.; Feng, R.; McLafferty, F. W. *Anal. Chem.* **1986**, *58*, 355–358.

[14] Frisch, M. J.; Head-Gordon, M.; Schlegel, H. B.; Raghavachari, K.; Binkley, J. S.; Gonzalez, C.; DeFrees, D. J.; Fox, D. J.; Whiteside, R. A.; Seeger, R.; Melius, C. F.; Baker, J.; Martin, R. L.; Kahn, L. R.; Stewart, J. J. P.; Fluder, E. M.; Topiol, S.; Pople, J. A. *GAUSSIAN 88*; Gaussian, Inc.: Pittsburgh, PA.

[15] (a) Møller, C.; Plesset, M. S. *Phys. Rev.* **1934**, *46*, 618. (b) Pople, J. A.; Binkley, J. S.; Seeger, R. *Int. J. Quantum Chem. Symp.* **1976**, *10*, 1–19.

Scheme II

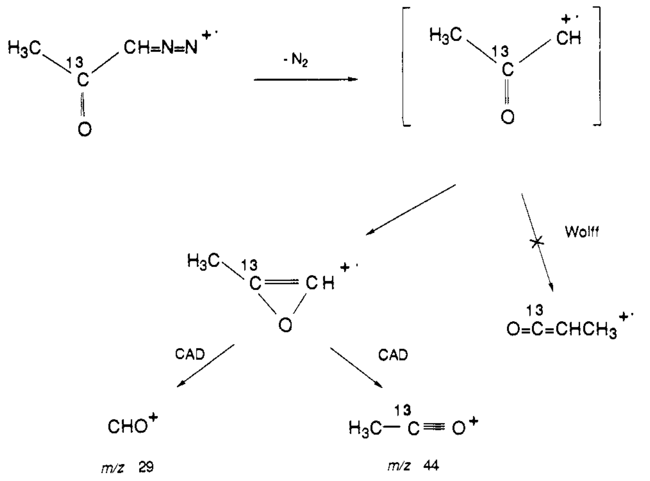

to in the text, and they correspond to relative energies at 0 K. The calculated harmonic vibrational frequencies were also used to calculate the 298 K relative energies which allowed comparison of the calculated and experimental thermochemical data. In addition, relative energies of several ion and neutral isomers and their isomerization barriers are estimated by semiempirical AM1 calculations.[16]

Results and Discussion

Methyloxirene Cation. Electron ionization (70 eV) of diazoacetone[17] gives rise to a $C_3H_4O^{\bullet+}$ ion (**a**) of 11% relative abundance. Unimolecular dissociation of metastable **a** (lifetime 13–16 μs) gives a Gaussian-type peak ($n = 2.35 \pm 0.06$)[18] of $C_3H_3O^+$ ($[C_3H_3O^+]/[\mathbf{a}] = 0.0082$) accompanied by large kinetic energy release ($T_{av} = 38 \pm 1$ kJ mol^{-1}). The collisionally activated dissociation (CAD)[19] spectrum of **a** (Figure 1) is different from those of the stable $C_3H_4O^{\bullet+}$ isomers, methylketene ($\mathbf{4}^{\bullet+}$),[20a] 2-propenal ($\mathbf{5}^{\bullet+}$),[20a] $^\bullet CH_2CH_2CO^+$,[20b] methyleneoxirane,[21] methoxyacetylene ($\mathbf{6}^{\bullet+}$), and 1-hydroxypropyne ($\mathbf{7}^{\bullet+}$). Besides an abundant $C_3H_3O^+$ ion, the CAD spectrum of **a** shows a conspicuous fragment at m/z 43 ($C_2H_3O^+$) due to loss of $CH^\bullet$, which is absent or extremely weak in the CAD spectra of the other $C_3H_4O^{\bullet+}$ isomers.[21] The loss of $CH^\bullet$ is unusual, but a CAD spectrum of **a** measured in the 4th field-free region[11b] (Table S1, supplementary material) also showed the $C_2H_3O^+$ peak excluding the possibility that this is an artifact from a metastably decomposing precursor.[23] The loss of $CH^\bullet$ is consistent with structures $\mathbf{1}^{\bullet+}$ or $\mathbf{3}^{\bullet+}$ that contain a terminal or ring CH group; $HC{\equiv}COCH_3^{\bullet+}$ ($\mathbf{6}^{\bullet+}$) is excluded because of its distinct CAD spectrum (Figure 1).

The ^{13}C-labeled **a** from [2-^{13}C]-diazoacetone shows clean shifts of m/z 43 to 44 and of m/z 41 to 42, indicating that the label is not scrambled among the skeletal carbon atoms. However, in the CAD spectrum of the labeled ion <5% of m/z 29 (CHO^+) is shifted to m/z 30 ($^{13}CHO^+$), showing that the oxygen atom is attached to a nonlabeled CH group (Scheme II); CHO^+ cannot be formed directly from structure $\mathbf{3}^{\bullet+}$. The presence of carbene structures ($\mathbf{2}^{\bullet+}$ or $\mathbf{3}^{\bullet+}$) in **a** was further examined through charge inversion by neutralization and reanionization ($^+NR^-$ spectra);[24] under these conditions other carbenes, such as $:CH_2$,[25] $:CHOH$,[24] $:C(CH_3)OH$,[26] and $:CHOCH_3$,[27] afford stable anion radicals, and α-ketocarbenes have been predicted to give stable anion radicals

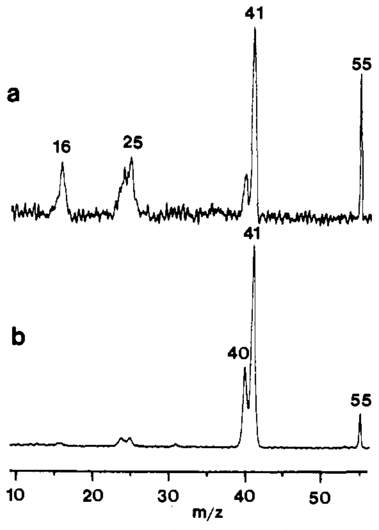

Figure 2. $^+NR^-$ spectra of (a) $\mathbf{1}^{\bullet+}$ and (b) $\mathbf{6}^{\bullet+}$.

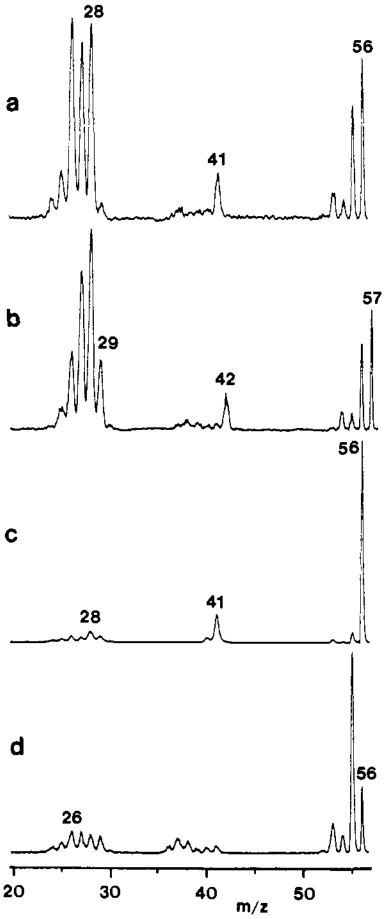

Figure 3. $^+NR^+$ mass spectra of (a) $\mathbf{1}^{\bullet+}$, (b) $(\mathbf{1}\text{-}^{13}C)^{\bullet+}$, (c) $\mathbf{6}^{\bullet+}$, and (d) $\mathbf{7}^{\bullet+}$.

---

(16) Dewar, M. J. S.; Zoebisch, E. G.; Eamonn, F.; Stewart, J. J. P. *J. Am. Chem. Soc.* **1985**, *107*, 3902–3909.

(17) Arndt, F.; Amende, J. *Chem. Ber.* **1928**, *61*, 1122–1125.

(18) Holmes, J. L.; Osborne, A. D. *Org. Mass Spectrom.* **1981**, *16*, 236.

(19) (a) McLafferty, F. W.; Bente, P. F., III; Kornfeld, R.; Tsai, S.-C.; Howe, I. *J. Am. Chem. Soc.* **1973**, *95*, 2120–2129. (b) McLafferty, F. W.; Kornfeld, R.; Haddon, W. F.; Levsen, K.; Sakai, I.; Bente, P. F., III; Tsai, S.-C.; Schuddemage, H. D. R. *J. Am. Chem. Soc.* **1973**, *95*, 3886.

(20) (a) Maquestiau, A.; Flammang, R.; Pauwels, P. *Org. Mass Spectrom.* **1983**, *18*, 547–552. (b) Traeger, J. C.; Hudson, C. E.; McAdoo, D. J. *Org. Mass Spectrom.* **1989**, *24*, 230–234.

(21) (a) Turecek, F.; Drinkwater, D. E.; McLafferty, F. W. *J. Am. Chem. Soc.* **1990**, *112*, 5892–5893. (b) Turecek, F.; Drinkwater, D. E.; McLafferty, F. W. *J. Am. Chem. Soc.* Preceding paper in this issue.

(22) Prepared by dissociative ionization of 2-butynoic acid (Aldrich), cf.: van Baar, B.; Weiske, T.; Terlouw, J. K.; Schwarz, H. *Angew. Chem., Int. Ed. Engl.* **1986**, *25*, 282–284.

(23) Schaldach, B.; Grützmacher, H.-F. *Org. Mass Spectrom.* **1980**, *15*, 166.

(24) Feng, R.; Wesdemiotis, C.; McLafferty, F. W. *J. Am. Chem. Soc.* **1987**, *109*, 6521–6522.

(25) Drinkwater, D. E.; Turecek, F.; McLafferty, F. W. Unpublished data.

(26) Wesdemiotis, C.; McLafferty, F. W. *J. Am. Chem. Soc.* **1987**, *109*, 4760–4761.

(27) Wesdemiotis, C.; Leyh, B.; Fura, A.; McLafferty, F. W. *J. Am. Chem. Soc.* **1990**, *112*, 8655–8660.

Table I. AM1 Heats of Formation and Zero-Point Vibrational Energies[a]

ion	$\Delta H_f°$	ZPVE
1$^{\bullet+}$	1043	154
2$^{\bullet+}$	980	148
3$^{\bullet+}$	1095	149
6$^{\bullet+}$	1014	155
7$^{\bullet+}$	928	152
TS (**1**$^{\bullet+}$→**2**$^{\bullet+}$)	1073[b]	145
TS (**1**$^{\bullet+}$→**3**$^{\bullet+}$)	1116[b]	145
TS (**3**$^{\bullet+}$→**6**$^{\bullet+}$)	1197[b]	133

[a] kJ mol^{-1}. [b] Saddle points with one imaginary frequency.

in solution.[28] However, the $^+$NR$^-$ spectrum of **a** (Figure 2, compared with the $^+$NR$^-$ of **6**$^{\bullet+}$) shows no detectable signal of $C_3H_4O^{\bullet-}$. These results are most compatible with the methyloxirene structure **1**$^{\bullet+}$ for **a**, which can form only a nonlabeled CHO^+ by direct ring cleavage and is expected to give an unstable anion radical (see below).

An MS/MS/MS experiment[10f,11b,29] was used to examine the dominant $C_3H_3O^+$ ion formed by CAD/O_2 of **a**. The CAD/He spectrum of these $C_3H_3O^+$ ions was identical (correlation coefficient, $r = 0.997$; Table S2, supplementary material) with that of the $CH_2{=}CHCO^+$ from methyl acrylate.[30] Thus the loss of the hydrogen atom from **1**$^{\bullet+}$ is accompanied by ring opening and hydrogen rearrangement to form the most stable $C_3H_3O^+$ isomer.[31] Of the other conceivable $C_3H_3O^+$ products, molecular orbital ab initio calculations predict $CH_2{=}C^+{-}CHO$ to be thermodynamically unstable and $CH_3C{=}C^+{-}O$ to be much less stable than $CH_2{=}CHCO^+$.[31] The formation of the latter from metastable **a** is nearly thermoneutral, $\Delta H_f°(CH_2{=}CHCO^+ + H^\bullet) = 969$ kJ mol^{-1}, $\Delta H_f°_{298}(\mathbf{1}^{\bullet+}) = 970$ kJ mol^{-1} (below and Table I); hence, the large kinetic energy release observed should be due to an isomerization energy barrier.

Neutral Methyloxirene. Collision with mercury of **1**$^{\bullet+}$ ions was used to generate the corresponding neutral species **1**. Mercury affords high yields of neutral products with little excitation by energy transfer.[12] Although the $^+$NR$^+$ mass spectrum (Hg, 70% transmittance/O_2, 50% transmittance) of **1**$^{\bullet+}$ (Figure 3) displays a significant survivor $C_3H_4O^{\bullet+}$ ion at m/z 56, the $C_2H_3O^+$ and CHO^+ ions characteristic of reionized **1**$^{\bullet+}$ are absent or of much lower relative intensity than those in the CAD spectrum of **1**$^{\bullet+}$. Consistent with the isomerization activation energy of ~8 kJ mol^{-1} for both oxirene[6] and dimethyloxirene,[5] methyloxirene formed by neutralization apparently undergoes extensive isomerization to more stable isomers, such as **4**,[21] **5**,[21] **6**, and/or **7**. Their $^+$NR$^+$ spectra are only qualitatively useful for isomeric characterization, as that of **1**$^{\bullet+}$ can contain ions formed by reionization of *neutral* **1**$^{\bullet+}$ dissociation products, and each of the isomerizations **1** → **4**–**7** is highly exothermic (see below). The most abundant fragment ions in the $^+$NR$^+$ spectrum of **4**$^{\bullet+}$ are m/z 28, 27, 26, and 41,[21] and $[m/z\ 29]/[m/z\ 28]$ is much lower than in the $^+$NR$^+$ spectra of **5**$^{\bullet+}$,[21] **6**$^{\bullet+}$, or **7**$^{\bullet+}$, consistent with their isomeric structures. Thus the $^+$NR$^+$ spectrum of **1**$^{\bullet+}$ indicates that neutralization is followed by fast isomerization **1** → **4**. However, the $(M - H)^+$ ion in the $^+$NR$^+$ spectrum of **1**$^{\bullet+}$ also points to minor formation of **5**,[21] and/or **7** (cf. Figure 3d). The $^+$NR$^+$ mass spectrum of **1**$^{\bullet+}$-^{13}C from $H_3C{-}^{13}CO{-}CHN_2$ (Figure 3) shows a peak at m/z 42 due to loss of the nonlabeled methyl group. The abundances in the C_2H_x + CO ion group at m/z 24–29 are consistent with 83% of the ^{13}C label present in the C_2H_x ions and only 17% in $CO^{\bullet+}$.[32] This indicates that most of the ^{13}C atoms originating from the precursor carbonyl group are *not* bonded to oxygen in the NR rearrangement products. This supports predominant isomerization of **1** to **2** (Scheme I, route b), which subsequently isomerizes to **4** (major, route e) and **5** or **7** (minor, routes f and g, respectively). This result is consistent with Zeller's conclusions on the Wolff rearrangement in photolysis of diazoacetone in solution.[3]

Theoretical Calculations and Thermochemical Data

This experimental evidence for the preferential isomerization of **1** to **4** via **2** does not answer the question of the competitiveness of the other isomerization paths shown in Scheme I; the intermediates involved (**1**, **2**, **3**), as well as some of the possible products, are too reactive under these experimental conditions. Therefore, the relevant parts of the $C_3H_4O^{\bullet+}$ and C_3H_4O potential energy surfaces were mapped by semiempirical AM1 calculations[16] (Table I; Table S3, supplementary material). These predict that the isomerization **3**$^{\bullet+}$ → **6**$^{\bullet+}$ requires 86 kJ mol^{-1}, but that **1**$^{\bullet+}$, **2**$^{\bullet+}$, and **3**$^{\bullet+}$ are stable equilibrium structures separated by very low barriers to isomerization. However, no experimental evidence was found for stable carbene ions **2**$^{\bullet+}$ and **3**$^{\bullet+}$, so that use of a higher level of theory was investigated. With geometry optimization of **3**$^{\bullet+}$ by ab initio calculations (6-31G* basis set),[33] the initial structure collapses at **1**$^{\bullet+}$. The latter ion is calculated at the MP4/6-31G*//6-31G* level[14] to be a stable equilibrium structure (Figure 4), 77 kJ mol^{-1} less stable than **5**$^{\bullet+}$, but 36 kJ mol^{-1} more stable than **6**$^{\bullet+}$. **2**$^{\bullet+}$ is also found to be an equilibrium structure (Figure 4), although destabilized against **1**$^{\bullet+}$ by 107 kJ mol^{-1}. The low stability of **2**$^{\bullet+}$ is consistent with our experiments and with previous calculations, indicating that the lower homologue of **2**$^{\bullet+}$, $HC{-}CHO^{\bullet+}$, is unstable, representing a transition state of the oxirene–ketene ion isomerization.[9] It should be noted that **1**$^{\bullet+}$, **2**$^{\bullet+}$, and **6**$^{\bullet+}$ are metastable with respect to dissociation to $C_2H_4^{\bullet+}$ and CO (Table II).

The AM1 potential energy diagram for the isomerizations of the *neutral* species (Figure 5) gives **1**, **2**, and **3** as high-energy structures separated from each other by low-energy barriers. The relative ordering of the transition-state energies for the isomerizations **1** → **2** and **1** → **3**, as well as **3** → **4**, **2** → **4**, and **2** → **5**, is qualitatively consistent with the experimental data, showing that the **1** → **2** → **4** route should be preferred. The AM1 energy for **1** was checked by ab initio calculations (MP4/6-31G*//6-31G* with 6-31G* zero-point vibrational energy corrections).[34] Propenal **5** was chosen as reference, since it is the only C_3H_4O isomer whose experimental heat of formation is well-established.[35] These higher level calculations give **1** as 292 kJ mol^{-1} less stable than **5**, in reasonable agreement with the AM1 relative energy ($\Delta E = 301$ kJ mol^{-1}, Figure 5). The total MP4 energies for **1** were essentially identical when based on equilibrium geometries obtained with the 6-31G* or 3-21G basis sets,[33,36] so the latter more economical basis set[36] was used for further ab initio calculations.

At the MP4/6-31G*//3-21G + ZPVE level of theory, **1** is marginally more stable than **2** and **3**. The isomerization paths for **1** → **2** and **1** → **3** were investigated in some detail by mapping the potential energy surfaces with 3-21G calculations (Figures 6 and 7). The **1** → **2** isomerization proceeds by stretching the C–O bond with negligible out-of-plane rotation of the methyl group (Figure 6). The reaction coordinate in the transition state also corresponds to C–O bond stretching, although the depth of the saddle with respect to methyl out-of-plane rotation is low (2.5 kJ mol^{-1}). By contrast, the **1** → **3** isomerization takes an early turn after moderate C–O bond stretching and passes a saddle point due to out-of-plane twisting of the C–H bond (Figure 7). Remarkably, in neither case do the reactions proceed by continuous

---

(28) Bethell, D.; Parker, V. D. *Acc. Chem. Res.* **1988**, *21*, 400–407.

(29) Burinsky, D. J.; Cooks, R. G.; Chess, E. K.; Gross, M. L. *Anal. Chem.* **1982**, *54*, 295–299. McLafferty, F. W., Ed. *Tandem Mass Spectrometry*; Wiley: New York, 1983.

(30) Holmes, J. L.; Terlouw, J. K.; Burgers, P. C. *Org. Mass Spectrom.* **1980**, *20*, 140–143.

(31) Bouchoux, G.; Hoppilliard, Y.; Flament, J.-P. *Org. Mass Spectrom.* **1985**, *20*, 560–564.

(32) This represents the best fit of the normalized relative intensities. Measured: m/z 25 (3.3), 26 (15.3), 27 (31.8), 28 (36.2), 29 (13.3), 30 (0.5); calculated m/z 25 (3.7), 26 (12.7), 27 (30.8), 28 (37.8), 29 (29 (14.7), 30 (0.3).

(33) Hariharan, P. C.; Pople, J. A. *Theor. Chim. Acta* **1973**, *28*, 213.

(34) Hehre, W. J.; Radom, L.; Schleyer, P. v. R.; Pople, J. A. *Ab Initio Molecular Orbital Theory*; Wiley: New York, 1986.

(35) Lias, S. G.; Bartmess, J. E.; Liebman, J. F.; Holmes, J. L.; Levin, R. D.; Mallard, W. G. *J. Phys. Chem. Ref. Data* **1988**, *17*, Suppl 1.

(36) Binkley, J. S.; Pople, J. A.; Hehre, W. J. *J. Am. Chem. Soc.* **1980**, *102*, 939–947.

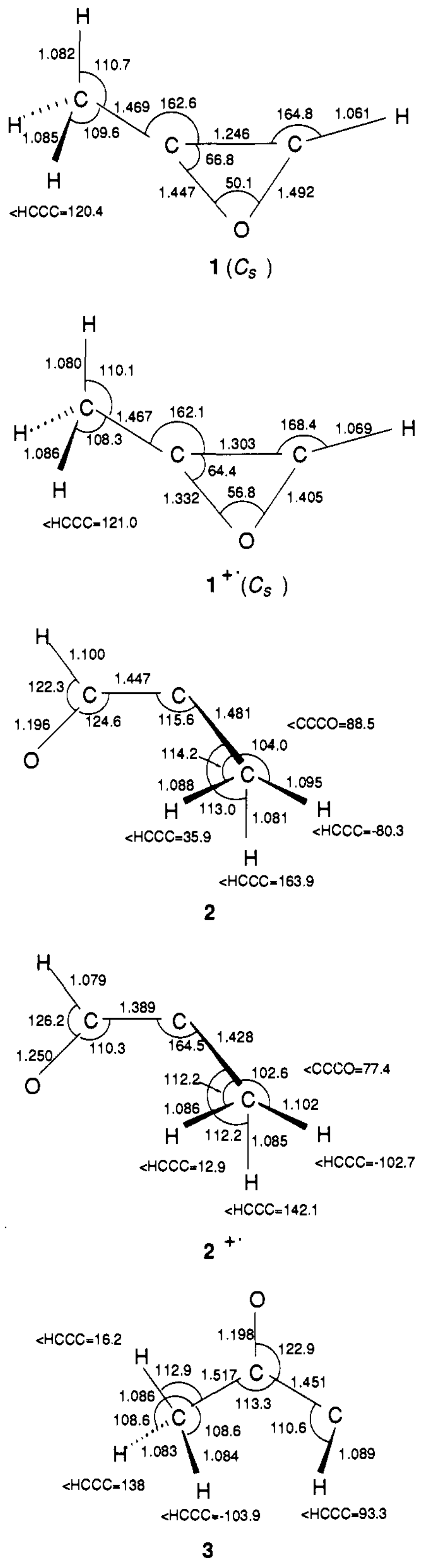

Figure 4. 6-31G* calculated equilibrium structures of $1^{\cdot+}$, $2^{\cdot+}$, 1, 2, and 3.

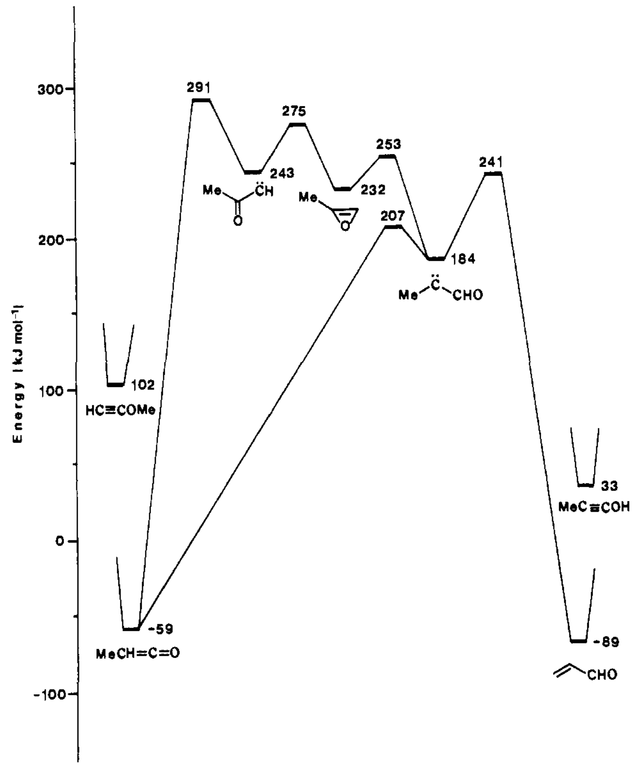

Figure 5. AM1 potential energy diagram for isomerizations of neutral C_3H_4O.

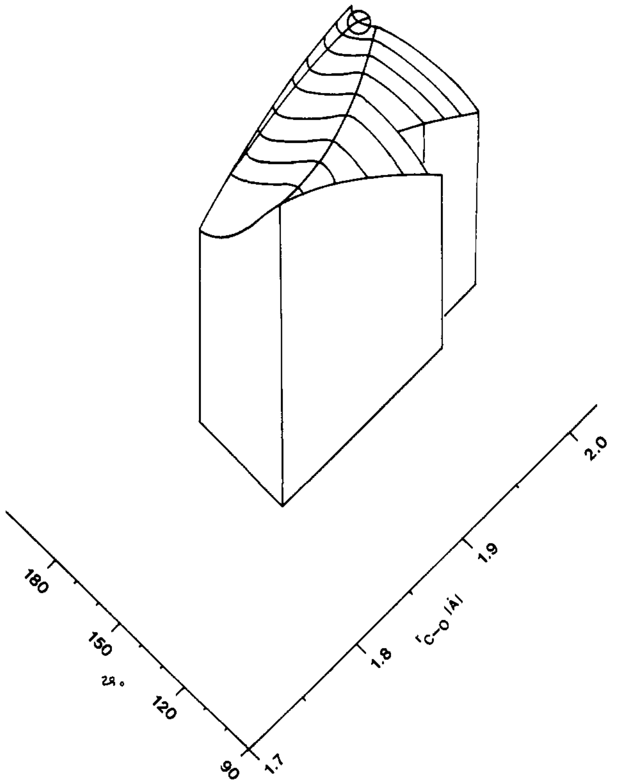

Figure 6. Partial 3-21G potential energy surface and saddle point (circle) for 1 → 2 isomerization. 1: $r_{C-O} = 1.447$ Å, CCCO dihedral angle, $\theta = 180°$. 2: $r_{C-O} = 2.405$ Å, $\theta = 88.5°$.

concerted mechanisms.[37] Instead both potential surfaces develop ridges at intermediate C–O bond stretchings and out-of-plane twisting. The height of the ridge diminishes as the C–O bond gets longer.

The isomerization barriers calculated at the 3-21G level are not numerically very much different from the AM1 values, although they show an opposite ordering. Unfortunately, our attempts to improve the relative transition-state energies by including the correlation energy via the Møller–Plesset perturbational treatment[15] met with little success, as the MP2, MP3, and MP4 energies diverged (Table III). In fact the MP4 transition-state energies dropped below those of the reactants. Obviously, a more extensive basis set or a multiconfigurational approach[38] will be

---

[37] For similar conclusions from ab initio calculations of reaction paths in small-ring openings see: Olivella, S.; Solé, A.; Bofill, J. M. *J. Am. Chem. Soc.* **1990**, *112*, 2160–2167.

Table II. Ab Initio Calculated Energies of $\mathbf{1}^{\bullet+}$, $\mathbf{2}^{\bullet+}$, and $\mathbf{6}^{\bullet+}$

	total energy^a						
ion	6-31G*	MP2	MP3	MP4	ZPVE^b	$E_{rel}{}^c$	$\Delta H_f{}^\circ{}_{298}{}^d$
$\mathbf{1}^{\bullet+}$	−190.396 289	−190.921 991	−190.942 043	−190.972 363	147.6	57.6	970
$\mathbf{2}^{\bullet+}$	−190.385 509	−190.865 251	−190.896 889	−190.929 482	141.8	164.3	1078
$\mathbf{6}^{\bullet+}$	−190.394 230	−190.904 693	−190.927 389	−190.958 641	151.2	97.2	1010^e

[a] 1 hartree = 2625.5 kJ mol^{-1}; 6-31G* optimized structures. [b] 6-31G* harmonic frequencies scaled by 0.9, kJ mol^{-1}. [c] MP4/6-31G* + 0.9 ZPVE, relative to $C_2H_4{}^{\bullet+}$ + CO.[20b] [d] Corrected for the 298 K heat contents with use of the scaled harmonic frequencies and referenced to $\Delta H_f{}^\circ{}_{298}$($CH_2{=}CHCHO^{\bullet+}$) = 898 kJ mol^{-1}.[35] [e] Reference 35 estimates the $\Delta H_f(\mathbf{6}^{\bullet+})$ as 989 kJ mol^{-1}.

Table III. Ab Initio Calculated Total and Relative Energies for the C_3H_4O System^a

	energy^b				
species	HF	MP2	MP3	MP4	ZPVE^c
1	−190.628 515 (0)	−191.196 939 (0)	−191.212 658 (0)	−191.246 522^d (0)	149.1
1^e	−190.616 651 (31)	−191.175 903 (55)	−191.194 225 (48)	−191.224 799 (57)	
2(singlet)	−190.656 915 (−75)	−191.186 503 (27)	−191.209 911 (7)	−191.242 600^d (10)	145.9
2(triplet)	−190.701 877 (−193)	−191.182 964 (37)	−191.215 701 (−8)	−191.242 414 (11)	146.9
3(singlet)	−190.654 625 (−69)	−191.183 805 (34)	−191.206 782 (15)	−191.239 796 (18)	145.4
3(triplet)	−190.700 361 (−189)	−191.184 108 (34)	−191.215 135 (−7)	−191.242 428 (11)	145.1
TS(**1**→**2**)	−190.621 031 (20)	−191.187 570 (25)	−191.196 009 (44)	−191.249 468 (−8)	144.8
TS(**1**→**3**)	−190.626 961 (4)	−191.196 587 (1)	−191.205 889 (18)	−191.254 957 (−22)	143.0

[a] Total energies in hartrees, relative energies (in parentheses) in kJ mol^{-1}. [b] 6-31G* single-point calculations on 3-21G optimized geometries. [c] kJ mol^{-1}; from 3-21G harmonic frequencies scaled by 0.9. [d] The corresponding MP4/6-31G*//6-31G* total energies were −191.245 453, −191.241 806, and −191.237 455 hartrees for **1**, **2**, and **3**, respectively. [e] Structure from vertical neutralization of the cation radical.

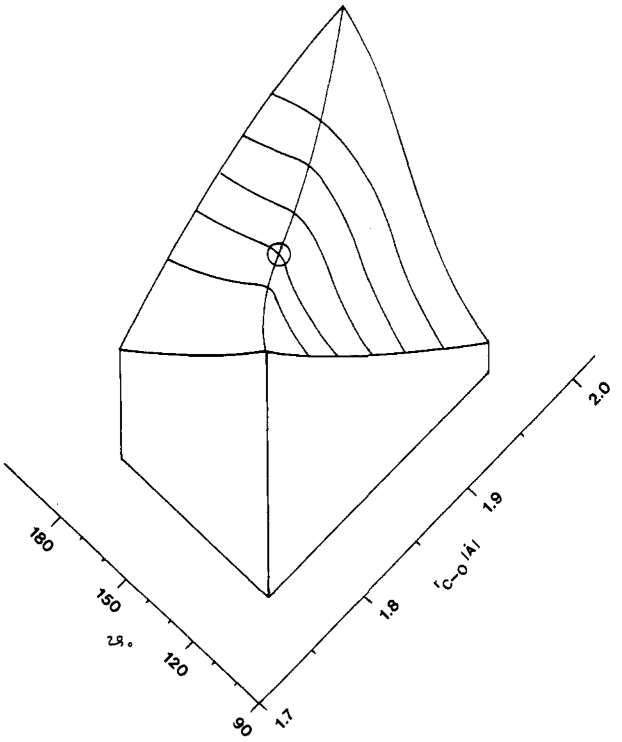

Figure 7. Partial 3-21G potential energy surface and saddle point (circle) for **1** → **3** isomerization. **3**: r_{C-O} = 2.426 Å, HCCC dihedral angle, θ = 93.3°.

necessary to obtain more realistic transition-state energies. In spite of these variations in the calculated energy values, it appears that the interconversion of **1**, **2**, and **3** must be very facile. By comparison, C–C bond shifts in substituted carbenes have been found to have activation energies of <15 kJ mol^{-1}.[39]

Since **1** is produced from the corresponding ion by vertical neutralization ($\tau \approx 10^{-15}$ s), the differences in the equilibrium geometries of the ion and the neutral can lead to vibrational excitation of the latter. Our MP4/6-31G*//6-31G* single-point-energy calculations for the neutral **1** formed with the $\mathbf{1}^{\bullet+}$ optimized geometry showed that the neutral gains 57 kJ mol^{-1} above the optimized structure **1** (Table III). In view of the low-energy barriers for **1** → **2** and **1** → **3**, such excitation should be quite sufficient to bring about fast isomerization.

Neutralization of cation radicals can produce triplet neutrals.[40] Although triplet **1** would represent a high-energy excited state, triplet carbenes **2** and **3** can be expected to be relatively stable species pertinent to the photochemical Wolff rearrangement.[3,4] Our calculations show comparable stabilities for triplets **2** and **3** versus their corresponding singlets (Table III). The small singlet–triplet gap in **2** and **3** contrasts the much larger ones (60 kJ mol^{-1}) calculated for the methylene–carbene system at a comparable level of theory.[41]

Conclusions

The stable methyloxirene cation radical $\mathbf{1}^{\bullet+}$ is formed by dissociative ionization of diazoacetone. Vertical neutralization of $\mathbf{1}^{\bullet+}$ yields the transient molecule **1** that isomerizes rapidly to methylformyl carbene and further to methylketene and propenal/or 1-hydroxypropyne. This supports the conclusions of previous solution studies.[3]

Acknowledgment. We gratefully acknowledge the generous financial support of the National Science Foundation (Grant CHE-8712039) and, for partial instrument funding, the National

---

(38) (a) Hegarty, D.; Robb, M. A. *Mol. Phys.* **1979**, *38*, 1795. (b) Sinanoglu, O.; Bruekner, K. A. *Three Approaches to Electron Correlation in Molecules*; Yale University: New Haven, CT, 1970.

(39) Moss, R. A.; Ho, G.-J.; Shen, S.; Krogh-Jespersen, K. *J. Am. Chem. Soc.* **1990**, *112*, 1638–1640.

(40) Sülzle, D.; Schwarz, H. *Chem. Phys. Lett.* **1989**, *156*, 397–400.

(41) Pople, J. A.; Frisch, M. J.; Luke, B. T.; Binkley, J. S. *Int. J. Quantum Chem. Symp.* **1983**, *17*, 307. For a review see: Shavitt, I. *Tetrahedron* **1985**, *41*, 1531–1542.

Institutes of Health (GM16609) and the computational support and technical assistance of the Cornell National Supercomputer Facility, which receives major funding from the National Science Foundation and the IBM corporation, with additional support from New York State and the Corporate Research Institute.

Supplementary Material Available: Tables of complete CAD spectra of $CH_2{=}CHCO^+$ and $C_3H_3O^+$, the fourth field-free spectrum of $1^{\cdot+}$, and the calculated harmonic vibrational frequencies (3 pages). Ordering information is given on any current masthead page.

Linkage Position Determination in Lithium-Cationized Disaccharides: Tandem Mass Spectrometry and Semiempirical Calculations

Gretchen E. Hofmeister,† Zhongrui Zhou, and Julie A. Leary*

Contribution from the College of Chemistry, University of California, Berkeley, California 94720.

Received January 7, 1991

Abstract: Fast atom bombardment ionization in combination with tandem mass spectrometry of lithiated disaccharides is used to differentiate the linkage position of five isomeric sugars. Labeling experiments in combination with product and precursor ion scans indicate that reducing ring opening occurs followed by two-, three-, and four-carbon cleavage. Carbonyl migration via keto–enol tautomerization is postulated as an isomerization that occurs during CID, thus enabling specific cleavages for each of the different isomers. Semiempirical calculations of both the hemiacetal and hydroxy aldehyde forms support experimental data that indicate that the lithium ion is pentacoordinate between the two rings.

Introduction

Fast atom bombardment (FAB) ionization combined with tandem mass spectrometry (MS/MS) has been exemplified as a method for determining both sequence and branching patterns of derivatized[1-3] and underivatized[4-6] oligosaccharides. Extensions of these studies include investigations of alkali-metal attachment to disaccharides and larger oligomers via different ionization techniques including laser desorption[7-11] as well as FAB[12,13] in an effort to better understand differences in fragmentation and stability of ions when alkali metals replace hydrogen in the cationic precursor. In a previous study, we reported preliminary data on linkage position determination when the dilithiated precursor of trisaccharides and tetrasaccharides was activated.[13] In order to better understand this phenomenon, we have investigated one isomer and subsequently applied this information to the other four isomeric disaccharides.

In this study, we show how the linkage position of different isomeric disaccharides can be distinguished when the monolithiated precursor undergoes collision-induced dissociation (CID) after FAB ionization. Deuterium- and ^{18}O-labeling studies were used to unambiguously determine where glycosidic cleavage is occurring. These labeling studies in conjunction with precursor and product ion scans show that specific reducing ring cleavage takes place when the monolithiated precursor of the various isomeric disaccharides undergoes CID. Since protonated molecular ions do not exhibit ring cleavage with FAB ionization and low-energy CID, the question of lithium-induced cleavage is addressed. Semiempirical calculations are also provided in an effort to better determine the position and extent of coordination of lithium to the molecule. The isomer gentiobiose (1,6-linked disaccharide) is investigated in detail, and mechanisms of fragmentation are postulated that are supported by experimental results and semiempirical calculations. These data are then applied to the 1,4, 1,3, 1,2, and 1,1 isomers, and the mechanism of fragmentation that gives information on linkage position is outlined.

Experimental Section

Collision-Induced Dissociation. Product ion spectra were generated from CID of the monolithiated molecular ions $(M + Li)^+$ transmitted into the quadrupole collision cell (q) of a BEqQ geometry instrument with 30–110-eV collision energy (laboratory frame of reference). Argon gas pressure ($1–2 \times 10^{-6}$ Torr) was measured with an ion gauge near the quadrupole collision cell. Low-energy CID spectra were obtained by scanning the mass analyzer up in mass from 50–400 u in 15–20 s, and 5–10 scans were acquired under data system control in the "MCA" (multichannel analyzer) mode. The mass scale of the quadrupole analyzer (Q) was calibrated by using low- and high-mass ions obtained from CID of the cluster ions of glycerol. Unit mass resolution was achieved for analysis of the isotopically labeled compounds, and was confirmed by obtaining resolution of the product ions at *m/z* 278 and 279 u of leucine–enkephalin.

Precursor Ion Scans. Precursor ion spectra were generated by scanning the magnet (B) while setting Q to pass only the mass of the product ion. This type of scan was again acquired under data system control with the mass range 100–500 u used for the front end scan.

Compounds. All disaccharides were purchased from Sigma Chemical Co. The deuterated compound gentiobiose-d_8 was prepared by dissolving 1 mg of disaccharide in 400 μL of D_2O (99.9% D, Cambridge Isotope Laboratories), and then lyophilizing the sample. This procedure was repeated three times, and then the sample was dissolved in 100 μL of D_2O to use as the stock solution. The ^{18}O-labeled gentiobiose compound was prepared by adding 0.5 μL of acetyl chloride to 1 mg of gentiobiose, dissolved in 100 μL of $^{18}OH_2$ (MSD, 97%, normalized for hydrogen

---

† Currently at the Department of Chemistry, M.I.T., Cambridge, MA 02139.

(1) Mueller, D. R.; Domon, B. M.; Blum, W.; Raschdorf, F.; Richter, W. J. *Biomed. Environ. Mass Spectrom.* **1988**, *15*, 441–446.

(2) Domon, B.; Mueller, D. R.; Richter, W. J. *Org. Mass Spectrom.* **1989**, *24*, 357–359.

(3) Domon, B.; Mueller, D. R.; Richter, W. J. *Biomed. Environ. Mass Spectrom.* **1990**, *19*, 390–392.

(4) Carr, S. A.; Reinhold, V. N.; Green, B. N.; Hass, J. R. *Biomed. Mass Spectrom.* **1985**, *12*, 288–295.

(5) Laine, R. A.; Pamidimukkala, K. M.; French, A. D.; Hall, R. W.; Abbas, S. A.; Jain, R. K.; Matta, K. L. *J. Am. Chem. Soc.* **1988**, *110*, 6931–6939.

(6) Garozzo, D.; Giuffrida, M.; Impallomeni, G.; Ballistreri, A.; Montaudo, G. *Anal. Chem.* **1990**, *62*, 279–286.

(7) Wright, L. G.; Cooks, R. G.; Wood, K. V. *Biomed. Mass Spectrom.* **1985**, *12*, 159–162.

(8) Spengler, B.; Dolce, J. W.; Cotter, R. J. *Anal. Chem.* **1990**, *62*, 1731–1737.

(9) Lam, Z.; Comisarow, M. B.; Dutton, G. G.; Weil, D. A.; Bjarnason, A. *Rapid Commun. Mass Spectrom.* **1987**, *1*, 83–86.

(10) Coates, M. L.; Wilkins, C. L. *Biomed. Mass Spectrom.* **1985**, *12*, 424–428.

(11) Coates, M. L.; Wilkins, C. L. *Anal. Chem.* **1987**, *59*, 197–200.

(12) Cerny, R. L.; Tomer, K. B.; Gross, M. L. *Org. Mass Spectrom.* **1986**, *21*, 655–660.

(13) Zhou, Z.; Ogden, S.; Leary, J. A. *J. Org. Chem.* **1990**, *55*, 5444–5446.

0002-7863/91/1513-5964$02.50/0